

Light Nuclei within Nuclear Matter

M. Beyer^{a,1} S.A. Sofianos^b N. Furutachi^c S. Oryu^c

^a *Institute of Physics, University of Rostock, 18051 Rostock, Germany*

^b *Department of Physics, University of South Africa, Pretoria 0003, South Africa*

^c *Department of Physics, Tokyo University of Science, Noda, Chiba 278-8510, Japan*

Abstract

We investigate the properties of ${}^3\text{He}$, ${}^4\text{He}$, ${}^6\text{He}$, ${}^7\text{Li}$ and ${}^{16}\text{O}$ nuclei in nuclear matter of finite temperature and density. A Dyson expansion of the many-body Green function leads to few-body equations that are solved using the Integro-Differential Equation Approach (IDEA) and the Antisymmetrized Molecular Dynamics (AMD) methods. The use of the latter method allows us to trace the individual movement of the wave packet for each nucleon and the formation and disintegration of quasi-nuclei in a changing thermodynamical nuclear matter environment.

PACS numbers: 21.45.+v, 21.60.Gx, 21.60.Jz, 21.65.+f

Keywords: Nuclear matter, correlations, clusters, finite temperature

Nuclear fragments detected in a heavy ion collision at intermediate energies play a central role to gain information on the properties and the dynamics of nuclear matter under extreme conditions. One particular interesting example is the liquid gas phase transition usually related to multi-fragmentation into light nuclei [1,2]. For more and other experiments see e.g. [3,4,5,6,7,8]. In practical calculations of heavy ion collisions [9,10,11,12,13,14,15,16,17,18,19], formation of clusters is described by kinematical (or geometrical) constraints that allow certain nucleons to combine to larger clusters or larger clusters to disintegrate. In some simulations these constraints are supplemented by a probability to occur that is either related to some fit parameter or in more microscopic approaches to the nucleon nucleon cross section. Depending on the specific approach, e.g. statistical multi-fragmentation models [9,10], microscopic transport models such as Boltzmann type [11,12,13,14,15], quantum molecular dynamics [16,17,18], or recent more intermediate type of event generators [19], the algorithms that deal with fragmentation are rather educated

¹ Corresponding Author: michael.beyer@uni-rostock.de, tel. +49 (381) 498 6773, fax. +49 (381) 498 6772

and powerful. Despite the decisive role of fragmentation, the exact conditions under which fragments are formed and which properties they have in such an excited nuclear many-body system are little known. In addition, even for a particular heavy ion collision at a given energy the formation of fragments could be at different stages under quite different conditions.

The parameters that are introduced into the simulation to accommodate fragmentation might be calculated microscopically. To motivate the objective of our present work we remind the reader how the conditions of deuteron formation are achieved in a microscopic statistical description of heavy ion collisions such as the Boltzmann-Uehling-Uhlenbeck (BUU) approach. To this end an overlap integral is introduced that cuts momentum components and hence geometrically describes the effect of Pauli blocking. To be more specific, formation of deuterons is only allowed if [11]

$$\int d^3q f \left(q + \frac{P_{\text{c.m.}}}{2} \right) |\phi(q)|^2 \leq F_{\text{cut}} \quad (1)$$

holds, where $P_{\text{c.m.}}$ denotes the c.m. momentum of the cluster and q the relative momentum of the nucleons inside the wave function $\phi(q)$ of the deuteron. The Pauli blocking is achieved by the nucleon momentum distribution function f . The cut-off F_{cut} is a parameter that needs to be fixed. Originally it has been treated as a fit parameter with a typical value of $F_{\text{cut}}^{\text{fit}} \simeq 0.2$. It has been shown that it is possible to connect this parameter to a microscopic calculation [14]. Using in-medium deuteron wave functions leads to $F_{\text{cut}} \simeq 0.15$ not quite the value used to fit to experiments. It could be that the higher value of $F_{\text{cut}}^{\text{fit}}$ simulates also evaporation from larger clusters that is not present in the microscopic approach used in [14]. The physical interpretation of (1) is due to the Mott transition that occurs when the binding energy of the cluster vanishes because of medium effects. For an early paper on a microscopic calculation of the deuteron's Mott transition see [20,21]. In the present work we proceed further along the pathway of Ref. [14] investigating the Mott transition for larger clusters up to ^{16}O using rigorous few-body equations that include the dominant medium effect, i.e. self energy corrections and Pauli blocking. This also extends previous investigations on the behavior of the nucleon deuteron reaction [14,22,23,24,25], the $^3\text{He}/^3\text{H}$ [26] and the α -particle [27,28] along this lines. These investigations were based on the Alt-Grassberger-Sandhas (AGS) equations [29] which were modified to include the effects of the medium.

Because of the Pauli blocking the effective interaction between nucleons becomes energy (E) dependent. To be specific we choose a temperature of $T = 10$ MeV that is characteristic for heavy ion collisions and also relevant for neutron stars. In the present work we first endeavor to transform the E -dependent nucleon-nucleon interaction to an E -independent one using the Marchenko inverse scattering method [30]. This paves the way to go beyond three- and

four-nucleon systems described by integral equations in momentum space by using configuration space formalisms. We employ here two such formalisms, namely the IDEA [31,32] and the AMD [33,34] methods. The former method is based on the assumption that the dominant correlations in the medium are still of two-body nature and thus one can obtain Faddeev-type equations for the corresponding two-body amplitudes. The AMD method, on the other hand, enable us to study changes in the density of the clusters embedded in the medium and obtain expectation values $\langle r \rangle$ for the center of the wave packets for each nucleon within the cluster. In our studies we consider, the ${}^3\text{He}$, ${}^4\text{He}$, ${}^6\text{He}$, ${}^7\text{Li}$ and the ${}^{16}\text{O}$ nuclei.

The Dyson expansion of the many-body Green function is used to obtain thermodynamic cluster Green functions for the A -nucleon system embedded in nuclear matter. The cluster Green functions are evaluated for an uncorrelated medium. Hence, they can be formulated as resolvents and respective resolvent equation can be derived for A quasi-nucleons that can be tackled with few-body techniques, however, modified effective potentials and self energies (masses). At a two body level this leads to the well known t -matrix equation [35],

$$T_2(z) = V_2 + V_2(1 - f_1 - f_2)R_0(z)T_2(z). \quad (2)$$

with $R_0(z) = (z - H_0)^{-1}$. The corresponding Schrödinger-type equation is

$$(H_0 - z)\Psi(12) + \sum_{1'2'}(1 - f_1 - f_2)V_2(12, 1'2')\Psi(1'2') = 0. \quad (3)$$

The f_i is the Fermi function given by

$$f_i = \frac{1}{e^{\beta(\varepsilon_i - \mu_{\text{eff}})} + 1} \quad (4)$$

with $\beta = 1/k_B T$. We have used an effective mass approximation, i.e. the quasi-particle energy ε is given by

$$\varepsilon = \frac{k^2}{2m} + \Delta_0^{\text{HF}}(k) \simeq \frac{k^2}{2m_{\text{eff}}} + \Delta_0^{\text{HF}}. \quad (5)$$

The constant shift Δ_0^{HF} can be absorbed in a redefinition of the chemical potential $\mu_{\text{eff}} = \mu - \Delta_0^{\text{HF}}$. For simplicity we take the effective masses used in previous calculations [14]. Assuming that the two-body system is at rest in the medium, then the kinetic energy term (3) is written as

$$H_0 = \frac{k_1^2}{2m_{\text{eff}}} = \frac{k_2^2}{2m_{\text{eff}}} = \frac{p^2}{2m_{\text{eff}}} = \frac{1}{2} E \quad (6)$$

while the effective interaction that appears in (2) and (3) is

$$V(E, r) = (1 - 2f(E)) V_2(r), \quad (7)$$

where $E = z - E_{\text{cont}}$ is the two-body center of mass energy. E_{cont} denotes the continuum edge as explained, e.g., in Ref. [20,21].

To transform this potential to an equivalent E -independent one, we employed the Marchenko inverse scattering method [30] which does not require to choose *a priori* the shape and range of the potential. The Schrödinger equation is transformed to an integral one for the non-local function $K(r, r')$,

$$K_\ell(r, r') + \mathcal{F}_\ell(r, r') + \int_r^\infty K_\ell(r, s) \mathcal{F}_\ell(s, r') ds = 0, \quad (8)$$

where the kernel $\mathcal{F}_\ell(r, r')$ is given by the Fourier transform of the S -matrix,

$$\begin{aligned} \mathcal{F}_\ell(r, r') = & \frac{1}{2\pi} \int_{-\infty}^{+\infty} h_\ell^{(+)}(kr) [1 - S_\ell(k)] h_\ell^{(+)}(kr') dk \\ & + \sum_{n=1}^{N_b} A_{n\ell} h_\ell^{(+)}(b_n r) h_\ell^{(+)}(b_n r'). \end{aligned} \quad (9)$$

In the above equation, $h_\ell^{(+)}(z)$ is the Riccati-Hankel function and $A_{n\ell}$ are the asymptotic normalization constants for the bound states $E_n = -\hbar^2/(2\mu) b_n^2$. The solution of Eq. (8) can then provide us the underlying local E -independent interaction $V(r)$.

$$V_\ell(r) = -2 \frac{dK_\ell(r, r)}{dr}. \quad (10)$$

More details and practical aspects of the method can be found in Ref. [36]. We only stress here that the Marchenko equation is fully equivalent to the Schrödinger equation. However, while in the latter equation one uses the knowledge of the potential from which the physical information of the underlying system can be extracted via the wave-function, in the Marchenko equation the information at hand is the scattering and bound state data embedded in the S -matrix.

An efficient way to study systems with $A \geq 3$ is to employ the IDEA method to the A -body. The method is based on Hyperspherical Harmonics and the A -body wave function, due to pairwise acting forces, can be written as a sum

of Faddeev-type amplitudes for the pairs (i, j) ,

$$\Psi(\mathbf{x}) = \sum_{i < j \leq A} \Phi(\mathbf{r}_{ij}, \mathbf{x}) = H_{[L_m]}(\mathbf{x}) \sum_{i < j \leq A} F(\mathbf{r}_{ij}, r), \quad (11)$$

where $H_{[L_m]}(\mathbf{x})$ is a harmonic polynomial of minimal degree L_m and r is the hyper-radius $r = (2/A) \sum_{i < j \leq A} r_{ij}^2$. Using (11) one obtains the Faddeev-type equation for the amplitude $F(\mathbf{r}_{ij}, r)$

$$(T - E) H_{[L_m]}(\mathbf{x}) F(\mathbf{r}_{ij}, r) = -V(r_{ij}) H_{[L_m]}(\mathbf{x}) \sum_{k < l \leq A} F(\mathbf{r}_{kl}, r). \quad (12)$$

This equation may be modified by introducing in both sides the average of the potential over the unit hypersphere, *i.e* the so-called hyper-central potential $V_0(r)$ [31,32] to obtain an integro-differential equation for the (modified) Faddeev amplitude $\phi(\mathbf{r}_{ij}, r)$. Furthermore, assuming that the radial motion and the orbital motion are nearly decoupled, we may write

$$\phi(\mathbf{r}_{ij}, r) = P(z, r)/r^{(D-1)/2} \approx P_\lambda(z, r)u_\lambda(r)$$

with $z = 2r_{ij}^2/r^2 - 1$ and one obtains the adiabatic approximation in which one extracts the potential surfaces $U_\lambda(r)$ that provide us with the binding energies and the scattering states of the system.

In contrast to the IDEA which is based on the Faddeev decomposition of the wave function, in the AMD method [33,34] one assumes that the antisymmetrized wave function for the A-nucleons is given by a Slater determinant

$$|\Phi(\mathbf{Z})\rangle = (1 \pm P)(1/\sqrt{A!}) \det [\varphi_{\mathbf{Z}_i}(\mathbf{r}_j)] \quad (13)$$

constructed from the the i -th nucleon wave function

$$\varphi_{\mathbf{Z}_i}(\mathbf{r}_j) \equiv \langle \mathbf{r}_j | \varphi_{\mathbf{Z}_i} \rangle | \chi_i \rangle = \left(\frac{2\nu}{\pi} \right)^{3/4} \exp \left[-\nu \left(\mathbf{r}_j - \frac{\mathbf{Z}_i}{\sqrt{\nu}} \right)^2 + \frac{1}{2} \mathbf{Z}_i^2 \right] | \chi_i \rangle. \quad (14)$$

In the above equations P is the parity projection operator, \mathbf{Z} is a set of (complex) parameters parameterizing the nucleon, $\mathbf{Z} = (\mathbf{Z}_1, \mathbf{Z}_2, \mathbf{Z}_3, \dots, \mathbf{Z}_A)$, ν is a width parameter for the wave packet and $|\chi_i\rangle = |\sigma_i \tau_i\rangle$ is the spin-isospin function for the nucleon i . To obtain the solution one employs the time dependent variational principle

$$\delta \int_{t_1}^{t_2} dt \frac{\langle \Phi(\mathbf{Z}) | [i\hbar \frac{d}{dt} - H] | \Phi(\mathbf{Z}) \rangle}{\langle \Phi(\mathbf{Z}) | \Phi(\mathbf{Z}) \rangle} = 0 \quad (15)$$

ρ (fm ⁻³)	³ He	⁴ He	¹⁶ O
0	8.67	30.7	1630
0.003	3.84	18.1	1280
0.007	0.75	8.56	979.6
0.009	—	5.70	874.8
0.017	—	—	628.0
0.034	—	—	507.8

Table 1

Binding energies (in MeV) in the eaa for ³He, ⁴He and ¹⁶O systems for different densities ρ (in fm⁻³)

where H is the total Hamiltonian of the system [33,34].

One of the main advantages of the AMD formalism is the possibility of tracing the momentum and position of the individual wave packet. For this one defines the harmonic oscillator annihilation operator

$$a = \sqrt{\nu}\mathbf{r}_i + \frac{i}{2\hbar\sqrt{\nu}}\mathbf{p}_i \quad \text{with} \quad a|\phi_{\mathbf{Z}_i}\rangle = \mathbf{Z}_i|\phi_{\mathbf{Z}_i}\rangle. \quad (16)$$

where \mathbf{Z}_i is a complex vector with its real and imaginary component are related to the average position and moment of the i -th wave packet,

$$\mathbf{Z}_i = \sqrt{\nu}\mathbf{D}_i + \frac{i}{2\hbar\sqrt{\nu}}\mathbf{K}_i \quad (17)$$

where

$$\mathbf{D}_i = \frac{\langle\phi_{\mathbf{Z}_i}|\mathbf{r}_i|\phi_{\mathbf{Z}_i}\rangle}{\langle\phi_{\mathbf{Z}_i}|\phi_{\mathbf{Z}_i}\rangle} \quad \text{and} \quad \mathbf{K}_i = \frac{\langle\phi_{\mathbf{Z}_i}|\mathbf{p}_i|\phi_{\mathbf{Z}_i}\rangle}{\langle\phi_{\mathbf{Z}_i}|\phi_{\mathbf{Z}_i}\rangle}. \quad (18)$$

In our calculations we employ the general form of the nucleon-nucleon potential

$$V(r) = (W + BP_\sigma - HP_\tau - MP_\sigma P_\tau)V(r) \quad (19)$$

where the bare potential $V(r)$ is the Volkov [37] interaction which is widely used in model nuclear structure calculations. We first employ the Wigner force only to study the influence of correlations on the bound states of ³He, ⁴He and of ¹⁶O for a various densities using the IDEA method. The binding energies obtained in the extreme adiabatic approximation (eaa) are given in Table 1. The ³He is the first to dissolve in the medium while the ¹⁶O still is bound

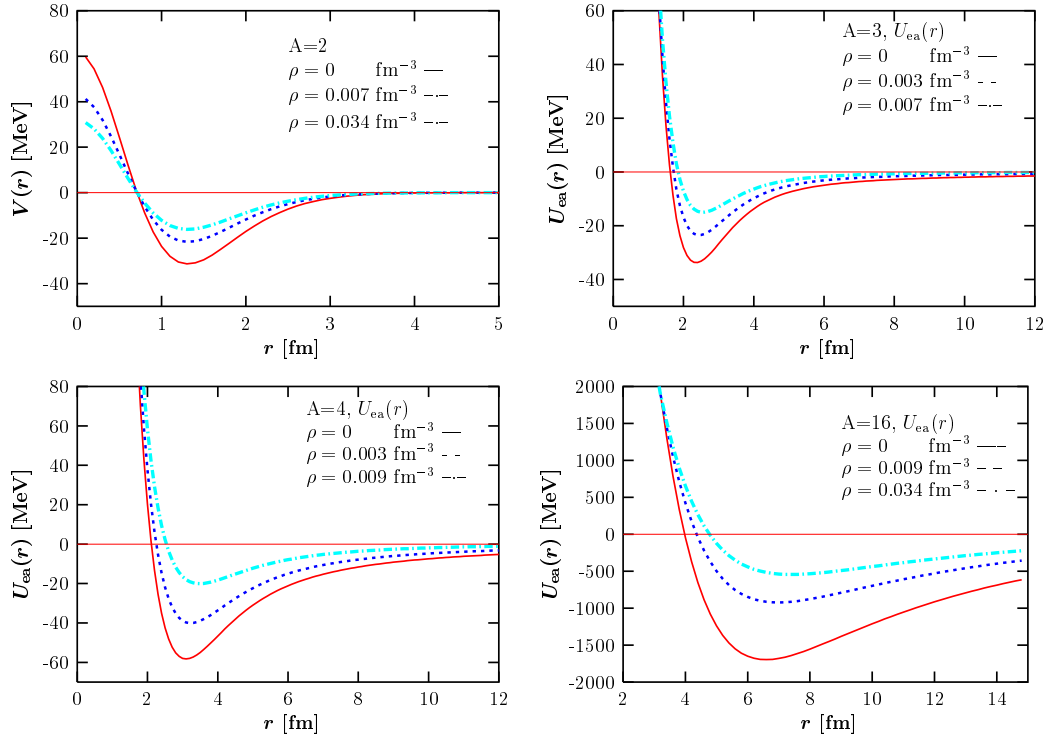


Fig. 1. The two-body potential and the potential surfaces (in the extreme adiabatic approximation) for $A = 3$, $A = 4$ and $A = 16$ for different densities ρ .

at the quite high density of $\rho = 0.034 \text{ fm}^{-3}$. Note, however, that already the isolated ^{16}O is strongly over-bound in the eaa. The disappearance of bound states is attributed to the weakening of the attraction in the interaction with increasing density ρ of the medium.

This can be seen in Fig. 1 where the potentials surfaces (in the eaa) are shown together with the two-body interaction. The weakening of the force can be seen also in Fig. 2 where the Faddeev components $P(r, z)$ are plotted for the ^4He case. For $\rho = 0.009 \text{ fm}^{-3}$ the component is quite flat with the maximum shifted to $\sim 5 \text{ fm}$ implying that the nucleons involved are already quite far from each other.

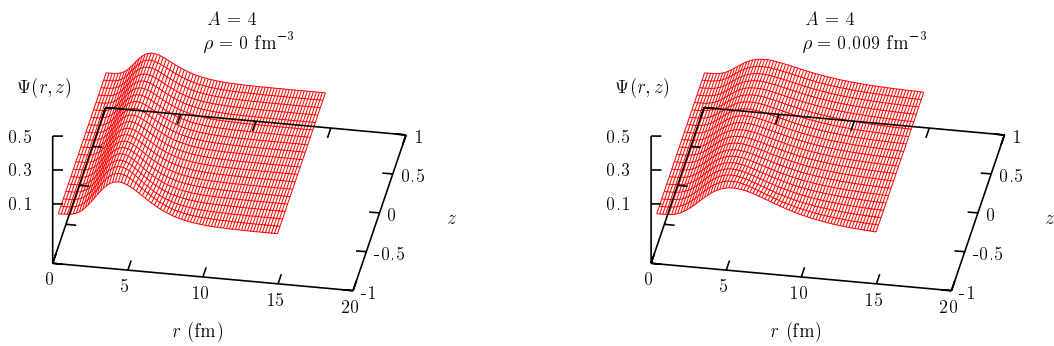


Fig. 2. The Faddeev components for the $A = 4$ system for $\rho = 0 \text{ fm}^{-3}$ and for $\rho = 0.009 \text{ fm}^{-3}$. The latter is just below the Mott density.

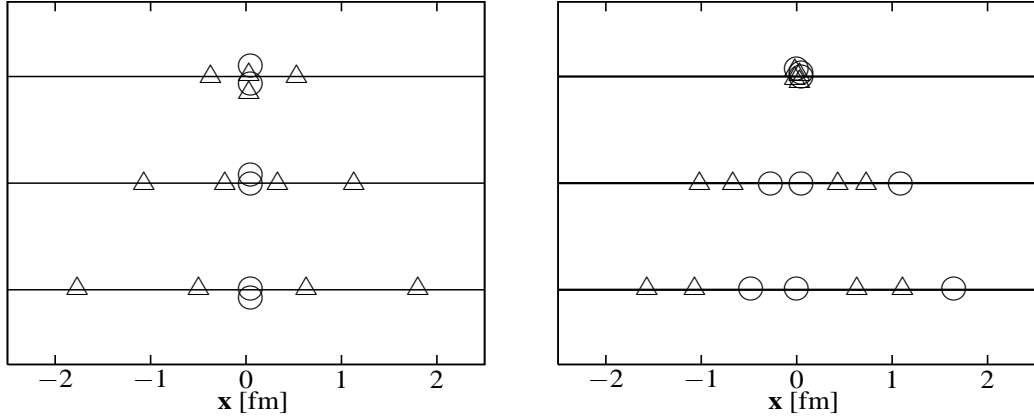


Fig. 3. Expectation values $\langle r \rangle$ for the center of the wave packets for protons (\circ) and neutrons (\triangle) for the ${}^6\text{He}$, left figure, and ${}^7\text{Li}$, right figure, with a Wigner force only. The three configurations (up to down) correspond to $\rho = 0 \text{ fm}^{-3}$, 0.009 fm^{-3} and 0.017 fm^{-3} respectively.

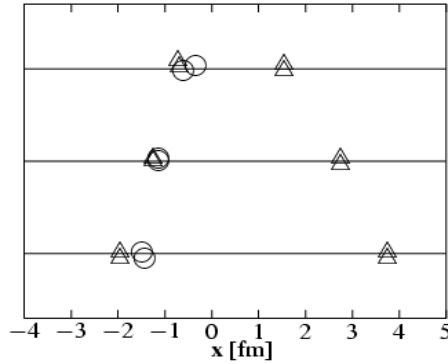


Fig. 4. Expectation values $\langle r \rangle$ for the center of the wave packets for protons (\circ) and neutrons (\triangle) for the ${}^6\text{He}$ with Majorana force included. The three configurations (up to down) correspond to $\rho = 0 \text{ fm}^{-3}$, 0.009 fm^{-3} and 0.017 fm^{-3} respectively.

As already mentioned, the main advantage of the AMD method is the possibility of tracing the movement of an individual proton or neutron by calculating the expectation value $\langle r \rangle$ for the corresponding wave packet. In Fig. 3 we show the results for the ${}^6\text{He}$ and ${}^7\text{Li}$ clusters with the Wigner force only. In the ${}^6\text{He}$ case the two neutrons are squeezed out of the cluster leaving the α -particle behind which, however, also is enlarged and ready to fall apart. The ${}^7\text{Li}$ is at first quite compact but two neutrons and a proton start to escape with increasing ρ and already at $\rho = 0.017 \text{ fm}^{-3}$ the 7 particles are not bound. It is interesting to note that although the α particle appears to be in the middle, the other particles always arranged themselves in an α particle formation.

The effects of the inclusion of the Majorana force in the calculation is shown in Fig. 4. The differences generated by the inclusion of this force is striking. The α particle acts as an attractive center for the two neutrons forming a

halo nucleus which are escaping with increasing ρ . In the case where only a Wigner force is considered, the two neutrons are escaping in either side of the α particle. However, the inclusion of spin-isospin component in the nuclear force generates two sub-clusters consisting of an α cluster and the two neutrons which tend to split first prior an overall disintegration occurs. These differences are best seen on the two-dimensional Fig. 5 obtained by integrating over the z -axis.

Our conclusions can be summarized as follows. i) The dynamical behavior of a nucleonic cluster in a medium can be reliably studied using a combination of methods namely, a cluster mean field approximation of the Dyson Green function expansion, an inverse scattering method for transforming the E -dependent potential to an E -independent one and few-body methods. ii) The construction of the E -independent interactions paves the way to study the behaviour of light nuclei ($A \sim 3-20$) in a medium using configuration space formalisms. iii) The use of the AMD method allows us to trace the individual movement of the nucleonic wave packet and the formation of sub-clusters when the density increases. This feature is particularly suited to explore correlations as has been done, e.g., for light clusters in a recent experiment [8], and also get insight into a possible evaporation mechanism of light clusters. iv) The use of Wigner forces alone seems to be insufficient for a proper description of the clusters while the inclusion of the Majorana force generated dramatic changes in the clustering picture of the particles. However, in order to obtain a complete picture on the behavior of quasi-nuclei in a changing nuclear matter environment, more realistic forces that include also the Bartlett and Heisenberg components as well as an LS-force should be employed. Although the effects of the former two components are expected to be small, the role played by the latter force in these extremely loose bound systems could be quite important and therefore its inclusion in studies concerning disintegration of clusters is warranted.

Acknowledgment

Financial support from the FRCCS of Tokyo University of Science to one of the author (SAS) is greatly acknowledged.

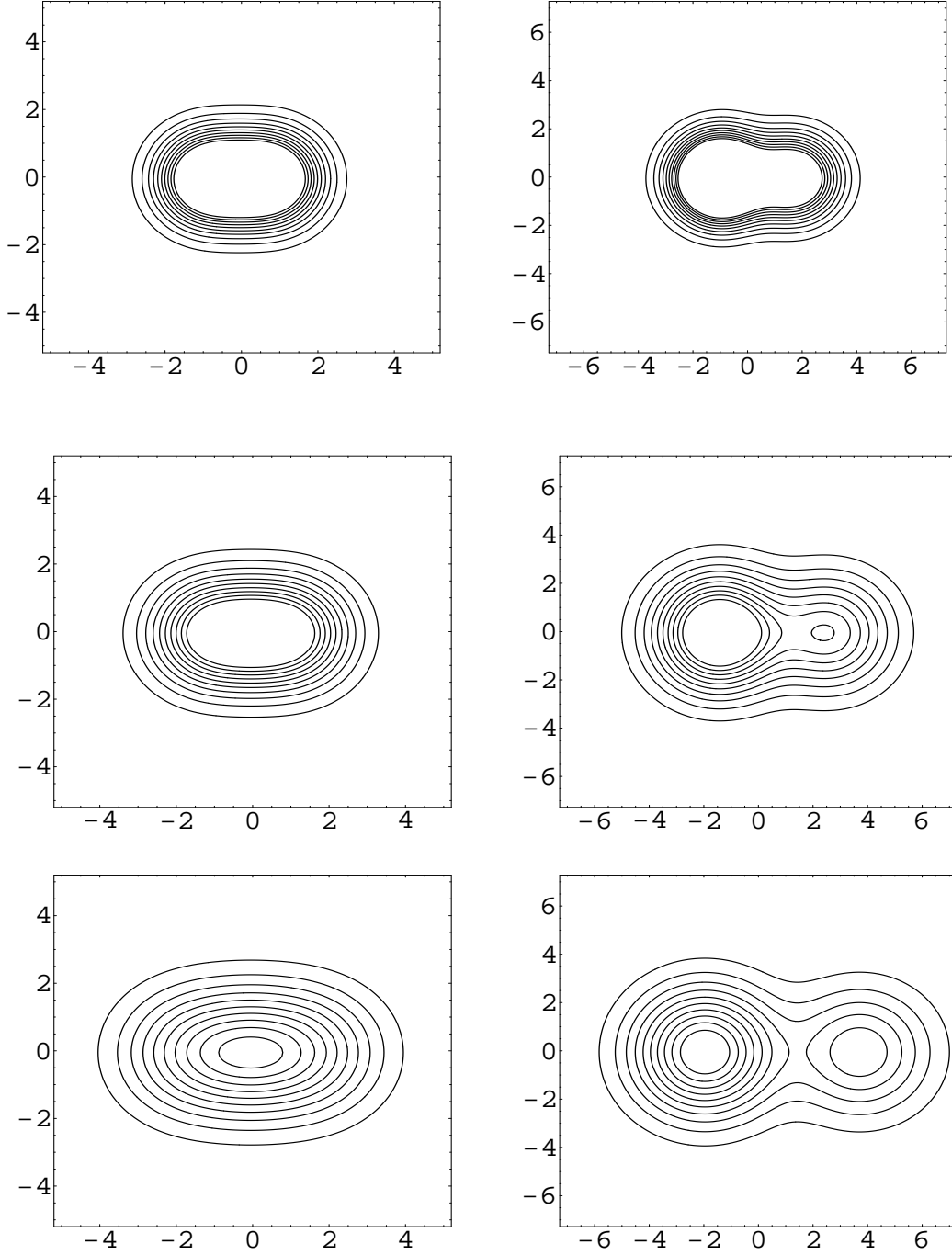


Fig. 5. Two-dimensional density plots for the ${}^6\text{He}$ system with a Wigner force (left panel) and with Majorana force included (right panel) for $\rho = 0 \text{ fm}^{-3}$, 0.007 fm^{-3} and 0.017 fm^{-3} (top to bottom). The figure scales are in fm. In the left panel the outermost line corresponds to the value of 0.01 fm^{-2} and gradually increases by 0.5 fm^{-2} until it reaches the value of 5 fm^{-2} for the innermost line. In the right panel the corresponding numbers are 0.01 fm^{-2} until 2 fm^{-2} in steps of $.2 \text{ fm}^{-2}$.

References

- [1] “Multi-fragmentation” eds. H. Feldmeier, J. Knoll, W. Norenberg and J. Wambach, proceedings, 27th International Workshop on gross properties of nuclei and nuclear excitations, Hirschegg, Austria, January 17-23, 1999,”
- [2] W. Trautmann, arXiv:nucl-ex/0411023.
- [3] INDRA Collaboration, B. Borderie *et al.*, Phys. Lett. B **353** (1995) 27.
- [4] INDRA Collaboration, B. Borderie *et al.*, Phys. Lett. B **388** (1996) 224.
- [5] R. Nebauer *et al.* [INDRA Collaboration], Nucl. Phys. A **658** (1999) 67.
- [6] INDRA Collaboration, D. Gorio *et al.*, Eur. Phys. J. A **7**, (2000) 245, and references therein.
- [7] S. Hudan *et al.* [INDRA Collaboration], Phys. Rev. C **67** (2003) 064613.
- [8] R. Ghetti *et al.*, arXiv:nucl-ex/0412038.
- [9] J. P. Bondorf, A. S. Botvina, A. S. Ilinov, I. N. Mishustin and K. Sneppen, Phys. Rept. **257** (1995) 133.
- [10] D. H. E. Gross, Rept. Prog. Phys. **53** (1990) 605.
- [11] P. Danielewicz and G. F. Bertsch, Nucl. Phys. A **533** (1991) 712.
- [12] P. Danielewicz and Q. Pan, Phys. Rev. C **46**, 2002 (1992).
- [13] H. Stocker and W. Greiner, Phys. Rept. **137** (1986) 277.
- [14] C. Kuhrts, M. Beyer, P. Danielewicz and G. Ropke, Phys. Rev. C **63** (2001) 034605.
- [15] M. Colonna, G. Fabbri, M. Di Toro, F. Matera and H. H. Wolter, Nucl. Phys. A **742** (2004) 337.
- [16] H. Feldmeier, Nucl. Phys. A **515** (1990) 147.
- [17] J. Aichelin, Phys. Rept. **202** (1991) 233.
- [18] R. Nebauer and J. Aichelin, Nucl. Phys. **A650**, 65 (1999); INDRA Collaboration, R. Nebauer *et al.*, Nucl. Phys. A658 (1999) 67.
- [19] D. Lacroix, A. Van Lauwe and D. Durand, Phys. Rev. C **69** (2004) 054604.
- [20] G. Röpke, L. Münchow and H. Schulz, Phys. Lett. **B 110** (1982) 21; Nucl. Phys. **A 379** (1982) 536.
- [21] M. Schmidt, G. Röpke and H. Schulz, Ann. Phys. (NY) **202** (1990) 57.
- [22] M. Beyer, G. Röpke and A. Sedrakian: Phys. Lett. **B 376** (1996) 7.
- [23] M. Beyer and G. Röpke, Phys. Rev. **C 56** (1997) 2636.

- [24] M. Beyer, *Few Body Syst. Suppl.* **10** (1999) 179.
- [25] C. Kuhrts, M. Beyer and G. Röpke, *Nucl. Phys. A* **668** (2000) 137.
- [26] M. Beyer, W. Schadow, C. Kuhrts and G. Röpke, *Phys. Rev. C* **60** (1999) 034004.
- [27] M. Beyer, S. A. Sofianos, C. Kuhrts ,G. Röpke and P. Schuck *Phys. Lett.* **B488** (2000) 247.
- [28] M. Beyer, S. Strauss, P. Schuck and S. A. Sofianos, *Eur. Phys. J. A* **22** (2004) 261.
- [29] E.O. Alt, P. Grassberger and W. Sandhas, *Nucl. Phys.* **B 2** (1967) 167.
- [30] Z. S. Agranovich and V. A. Marchenko *The Inverse Problem of Scattering Theory*, (Gordon & Breach, New York, 1964)
- [31] M. Fabre de la Ripelle, H. Fiedeldey and S. A. Sofianos, *Phys. Rev., C* **38** (1988) 449.
- [32] M. F. de la Ripelle, S. A. Sofianos and R. M. Adam, arXiv:nucl-th/0410016 (accepted for publication in *Annals of Physics*).
- [33] A. Ono, H. Horiuchi, T. Maruyama and A. Ohnishi, *Prog. Theor. Phys.* **87** (1992) 1185; Y. Kanada-En'yo, H. Horiuchi and A. Ono, *Phys. Rev. C* **52** (1995) 628; Y. Kanada-En'yo and H. Horiuchi *Phys. Rev. C* **52** (1995) 647;
- [34] T. Watanabe, Y. Taniguchi, N. Sawado and S. Oryu *Modern Physics Letters* **18** (2003) 182; Y. Taniguchi, T. Watanabe, N. Sawado and S. Oryu *Few-Body Systems Suppl.* **15** (2003) 247.
- [35] For a textbook treatment see, e.g., A. L. Fetter, J.D. Walecka, *Quantum Theory of Many-Particle Systems*, (Mc Graw-Hill, New York, 1971), and Dover reprints 2003.
- [36] S. E. Massen , S. A. Sofianos, S. A. Rakityansky, and S. Oryu 2000 *Nucl. Phys.* **A 654** (2000) 597.
- [37] A. B. Volkov, *Nucl. Phys.* **74** (1965) 33.